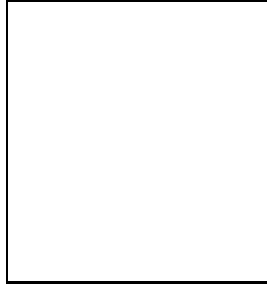


# LOOKING FOR CLUES TO THE NATURE OF HI DEFICIENCY IN CLUSTER SPIRALS <sup>a</sup>

J.M. SOLANES

*Departament d'Enginyeria Informàtica i Matemàtiques, Universitat Rovira i Virgili.  
Carretera de Salou, s/n; E-43006 Tarragona, Spain*



We derive the atomic hydrogen content for 1900 spirals in the fields of eighteen nearby clusters. By comparing the HI deficiency distributions of the galaxies inside and outside one Abell radius ( $R_A$ ) of the center of each region, we find that two thirds of the clusters in our sample show a dearth of neutral gas in their interiors. Possible connections between the gaseous deficiency and the characteristics of both the underlying galaxies and their environment are investigated in order to gain insight into the cause of HI depletion. In the clusters in which neutral gas deficiency is pronounced, we see clear indications that the amount of depletion is related to the morphology of the galaxies: early-type and, probably, dwarf spirals are more easily emptied of gas than the intermediate Sbc–Sc types. Gas contents below one tenth, and even one hundredth, of the expected value have been measured, implying that gas removal must be very efficient. Our 21-cm data also show that in the HI-deficient clusters the proportion of gas-poor spirals decreases continuously towards the outskirts of these systems, the zone of significant deficiency reaching as far out as  $2R_A$ . In an independent analysis of the Virgo cluster, we find suggestive indications that gas losses are driven by the interaction of the disks with the inner hot intracluster gas around M87. We also report evidence that gas-poor spirals follow more radial orbits than those of the gas-rich objects. We conclude that ISM-IGM hydrodynamic effects appear as the most plausible cause of HI removal.

## 1 The Cluster Sample

The galaxies used in the present study have been extracted from the all-sky database of nearby galaxies maintained by R. Giovanelli and M.P. Haynes known as the Arecibo General Catalog (AGC). To be assigned to a given cluster field, a galaxy must lie within a projected distance of  $5R_A$ , i.e. within  $7.5 h^{-1}$  Mpc, of the cluster center and have a radial velocity which is separated

<sup>a</sup>For further details, see J.M. Solanes, A. Manrique, C. García-Gómez, G. González-Casado, R. Giovanelli, and M.P. Haynes, *Astrophysical Journal*, in press (2000); astro-ph/0007402.

Table 1: Cluster Fields

Name	R.A. (1950)			Dec. (1950)			Velocity Filter ( $\text{km s}^{-1}$ )	$R_A$ (deg)	# of Galaxies		$P_{KS}$
	(h)	(m)	(s)	( $^{\circ}$ )	( $\iota$ )	( $\prime$ )			$r \leq 1R_A$	$r \leq 5R_A^b$	
Pisces	00	59	54.0	+30	02	00	3500÷7500	1.88	14	155	0.316
N507	01	24	26.8	+34	03	35	3500÷7500	1.83	19	124	0.497
A262	01	49	49.9	+35	53	50	3000÷7000	1.90	35	168	0.002
A397	02	53	51.2	+15	41	35	8500÷11000	0.95	10	26	0.003
A400	02	55	00.0	+05	48	25	5000÷9000	1.28	33	100	0.057
A426	03	16	30.0	+41	20	00	2000÷9000	1.70	12	99	0.008
A539	05	13	55.2	+06	23	16	6500÷10500	1.03	22	38	0.909
Cancer	08	17	00.0	+21	11	00	2500÷7000	1.75	17	83	0.581
A779	09	16	44.3	+33	57	18	4500÷9000	1.25	11	28	0.012
A1060	10	34	27.7	-27	16	26	2000÷5500	2.16	20	96	0.060
A1367	11	42	04.6	+19	59	14	4000÷9000	1.32	28	100	<0.001
Virgo	12	28	18.0	+12	40	00	-500÷2700	7.23	218	426	<0.001
A3526	12	46	06.0	-41	02	00	1400÷4500	2.54	12	76	0.491
A1656	12	57	18.3	+28	12	22	4000÷10000	1.25	25	100	<0.001
A2063	15	20	39.1	+08	47	18	9000÷12000	0.84	11	21	0.004
A2147	15	59	58.3	+16	06	15	8000÷14000	0.86	21	57	0.002
A2151	16	02	22.0	+17	51	48	8000÷14000	0.82	25	58	0.405
Pegasus	23	18	00.0	+07	55	00	2000÷5500	2.36	25	145	0.011

<sup>b</sup>For the Virgo cluster the maximum radial cutoff is  $3R_A$ .

from the recessional velocity of the cluster no more than  $\sim 3$  times its average velocity dispersion. Since we are especially interested in the central portions of clusters where environmental influences are strongest, we have only selected those clusters with at least 10 galaxies (of types Sa–Sdm/Irr) with good HI detections located within the innermost  $1R_A$  ( $1.5 h^{-1}$  Mpc) radius circle.

HI deficiencies for individual galaxies have been quantified by means of a parameter DEF that compares, the observed HI mass,  $h^2 M_{\text{HI}}^{\text{obs}}$ , in solar units, with the value expected from an isolated (i.e. free from external influences) galaxy of the same morphological type,  $T^{\text{obs}}$ , and optical linear diameter,  $hD_{\text{opt}}^{\text{obs}}$ , expressed in kpc (for details, see Haynes and Giovanelli<sup>1</sup>):

$$\text{DEF} = \langle \log M_{\text{HI}}(T^{\text{obs}}, D_{\text{opt}}^{\text{obs}}) \rangle - \log M_{\text{HI}}^{\text{obs}}, \quad (1)$$

so positive values of DEF indicate HI deficiency. For the expectation value of the (logarithm of the) HI mass, we use the maximum likelihood linear regressions of  $\log(h^2 M_{\text{HI}})$  on  $\log(hD_{\text{opt}})$  inferred from isolated galaxies by Solanes *et al.*<sup>2</sup> Because the standards of normalcy for the HI content are well defined only for the giant spiral population (Sa–Sc), we have excluded from the present study earlier Hubble types, as well as all galaxies unclassified or with peculiar or very disturbed morphologies. Nonetheless, HI mass contents for the few HI-rich Sd’s, Sdm’s, and Magellanic-type irregulars included in our samples have been calculated from the relationship inferred for the Sc’s.

We have selected from the AGC a total of eighteen cluster fields (see Table 1). These are the sky regions centered on the ACO clusters A262, A397, A400, A426 (Perseus), A539, A779, A1060 (Hydra I), A1367, A1656 (Coma), A2063, A2147, A2151 (Hercules), and A3526 (Centaurus30), on the clusters of Virgo, Pegasus, Cancer, and Pisces, and on the group of galaxies around NGC507, hereinafter referred to as N507. Figure 1 shows the histograms of the distribution of the measured values of DEF according to equation (1) for these same regions. In the histograms, the filled areas illustrate the distribution for the galaxies within  $1R_A$ —for which we adopt the cluster distance—, while the unfilled areas correspond to those objects at larger radii. Apart

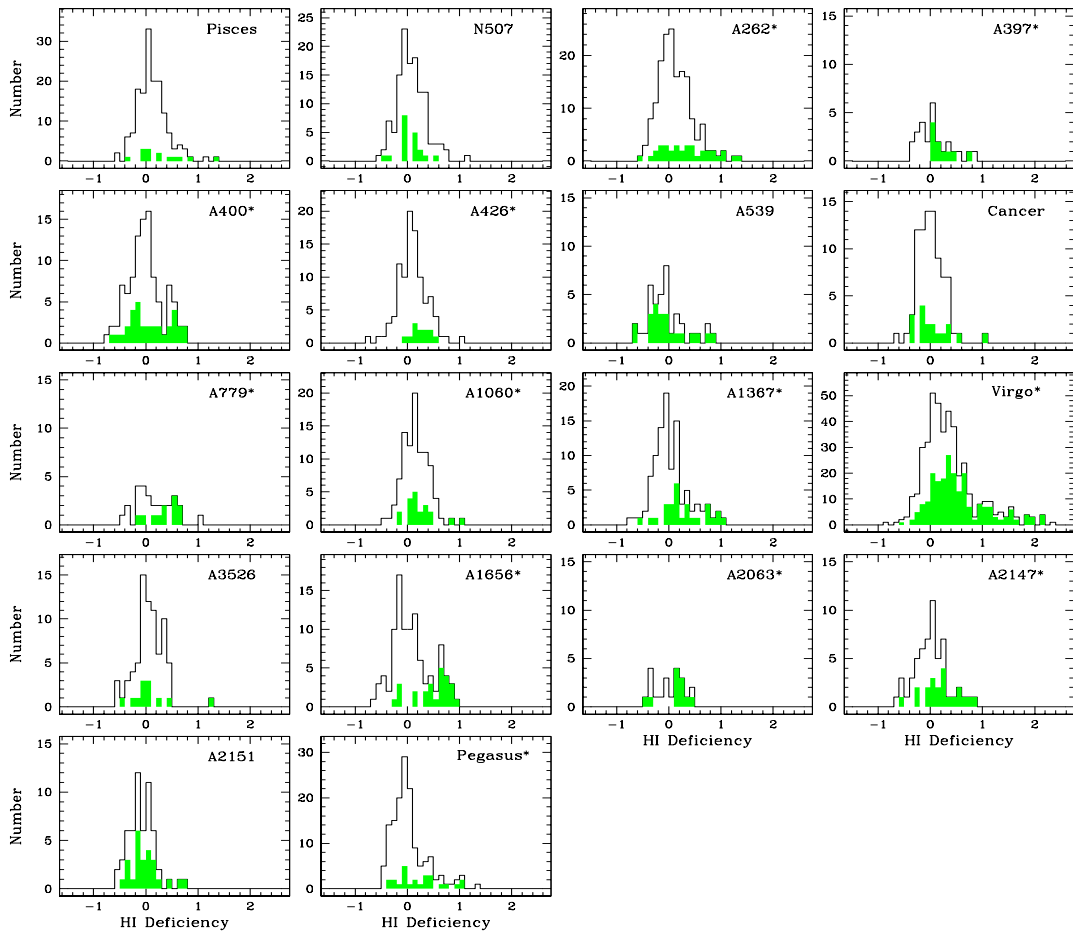


Figure 1: Histograms showing the distribution of the computed HI deficiency parameter DEF for each cluster region. In each panel the filled portions of the histogram indicate deficiencies for galaxies located within  $1R_A$  of the cluster center, while the unfilled areas represent galaxies at larger radii. HI-deficient clusters are identified by an asterisk after the name.

from some expected contamination by outliers, it is evident from this latter figure that, while the outer distributions tend to be bell-shaped, exhibit a dispersion comparable to the value of 0.24 measured for isolated galaxies,<sup>2</sup> and peak around zero DEF, the central galaxies of the majority of the clusters show evidence for strong HI deficiency. The most notable case is that of Virgo, for which some of the inner galaxies have HI masses up to two orders of magnitude below their expectation values. Some samples include a few galaxies undetected in HI but for which a reliable upper limit of their HI content has been calculated. In the calculations of DEF made through this paper, non-detections always contribute with their nominal lower limit of deficiency.

We choose to define a cluster as HI deficient when a two-sample Kolmogorov-Smirnov (KS) test gives a probability of less than 10% that its observed inner and outer distributions of DEF are drawn from the same parent population. The results of the KS test confirm essentially the visual impression: the central spiral populations of twelve cluster fields, Pegasus, Virgo, A262, A397, A400, A426, A779, A1060, A1367, A1656, A2063, and A2147 (identified in Fig. 1 by an asterisk after the name) have statistically significant reduced HI contents. For the other six galaxy concentrations, Cancer, N507, Pisces, A539, A2151, and A3526, the presence of objects with large HI deficiencies in the central regions is an exception of the norm. The results of the

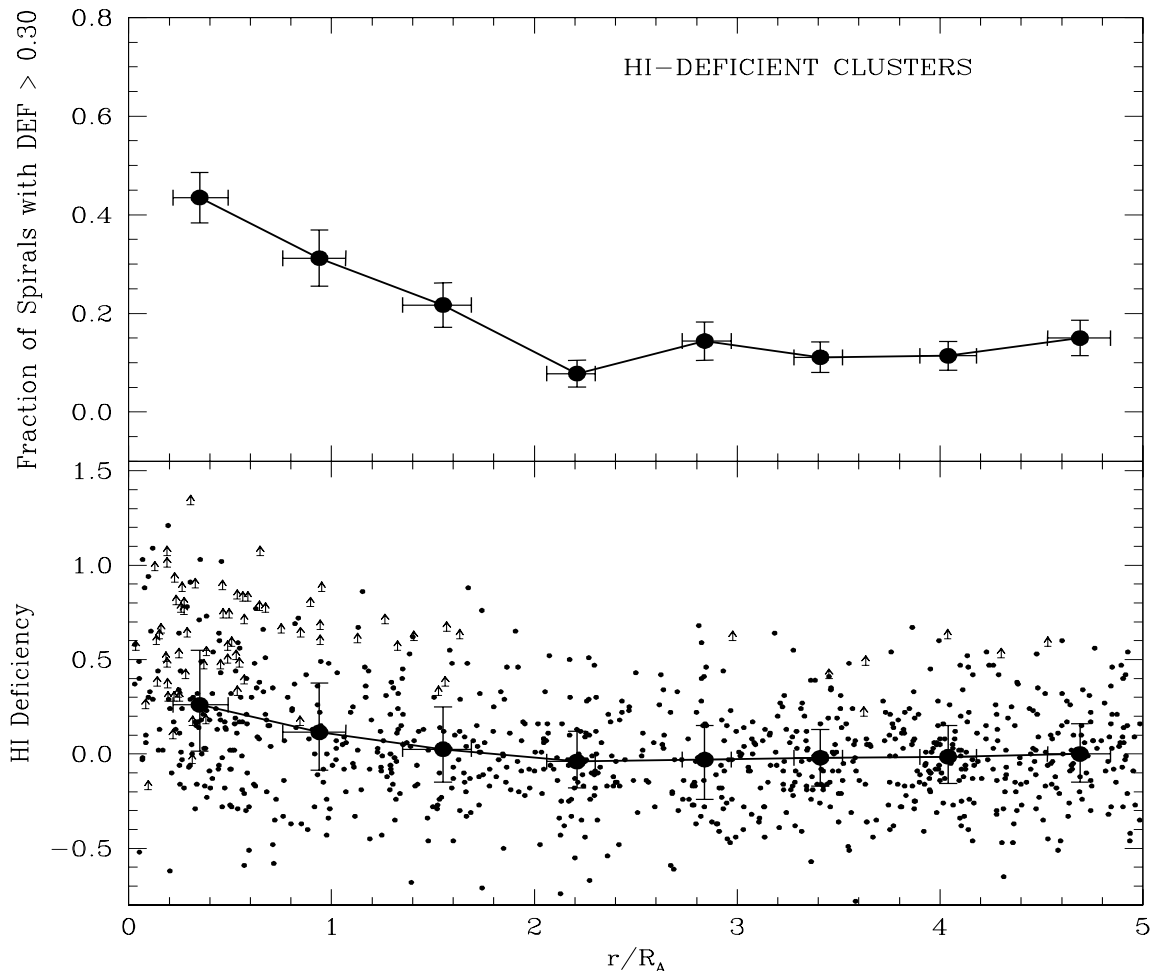


Figure 2: *Top*: HI-deficient fraction in bins of projected radius from the cluster center for the superposition of all the HI-deficient clusters but Virgo. *Bottom*: same in upper panel for the measured HI deficiency. Small dots show the radial variation of HI deficiency for individual galaxies while the arrows identify non-detections plotted at their estimated lower limits.

KS test are listed in the last column of Table 1.

## 2 The Spatial Pattern of HI Deficiency

### 2.1 The Radial Variation of HI Deficiency

A well-known property of the HI deficiency pattern in clusters is its radial nature. In order to obtain a precise characterization of the radial behavior of HI deficiency we have combined into a single dataset the HI measures for spirals in all the clusters which show HI deficiency other than Virgo, with their clustercentric distances normalized to  $1R_A$ . This composite sample of eleven HI-deficient clusters allows us to trace deficiency out to projected distances from the cluster center of  $5R_A$  in much greater detail than the (relatively) small samples of the individual clusters, while at the same time reduces possible distortions caused by substructure and asphericity. Virgo is excluded from this composite cluster because of its smaller radial extent and the fact that its much larger dataset would dominate the composite cluster. To characterize gas removal we adopt a measure based on the relative populations of deficient and normal spirals, which has a reduced sensitivity to the presence of censored data. In Figure 2, we show the variation in the

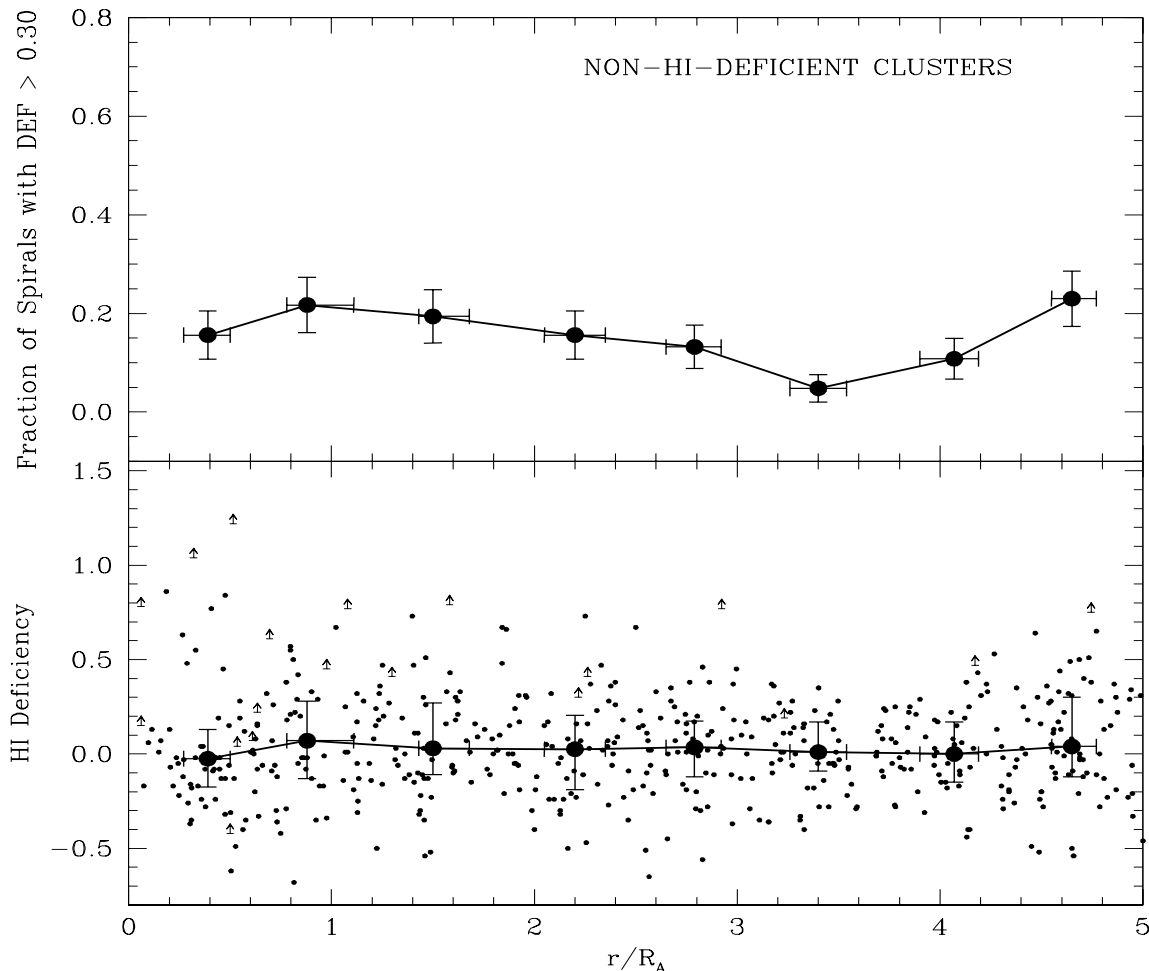


Figure 3: Same as in Figure 2 but for the superposition of all the non-HI-deficient clusters.

fraction of spirals with  $\text{DEF} > 0.30$  per bin of projected radial distance, in Abell radius units, for our composite HI-deficient cluster. The radial dependence of HI deficiency is clearly evident for  $r < 2R_A$ : the percentage of gas-poor spirals increases monotonically up to the center. Beyond this projected distance, however, the fraction of gas-deficient disks remains constant around a value of  $\sim 10\text{--}15\%$ , a value consistent with the fraction of field spirals with  $\text{DEF} > 0.30$  expected from a Gaussian distribution of values of this parameter with an average dispersion of 0.24.<sup>2</sup> We have also included in Figure 2 a second panel showing the variation of HI deficiency with projected radius. It provides visual verification of the fact that, at large clustercentric distances where gas-deficient galaxies are scarce and the contribution of non-detections negligible, the distributions of HI content at different radii are in excellent agreement both in terms of location and scale with that of field galaxies. This latter result supports further the statistical reliability of our measures of DEF through eq. (1). The same two previous plots are repeated in Figure 3 for the superposition of the clusters which are not deficient in HI.

It is clear from Figure 2 that the influence of the cluster environment on the neutral gas content of galaxies can extend beyond one Abell radius (plots of the radial variation of HI deficiency for individual clusters, not shown here, indicate that the extent of the zone of significant HI deficiency fluctuates significantly from cluster to cluster). In this one respect, it is interesting to note that Balogh *et al.*,<sup>3</sup> using [OII] equivalent width data, have found that the mean star

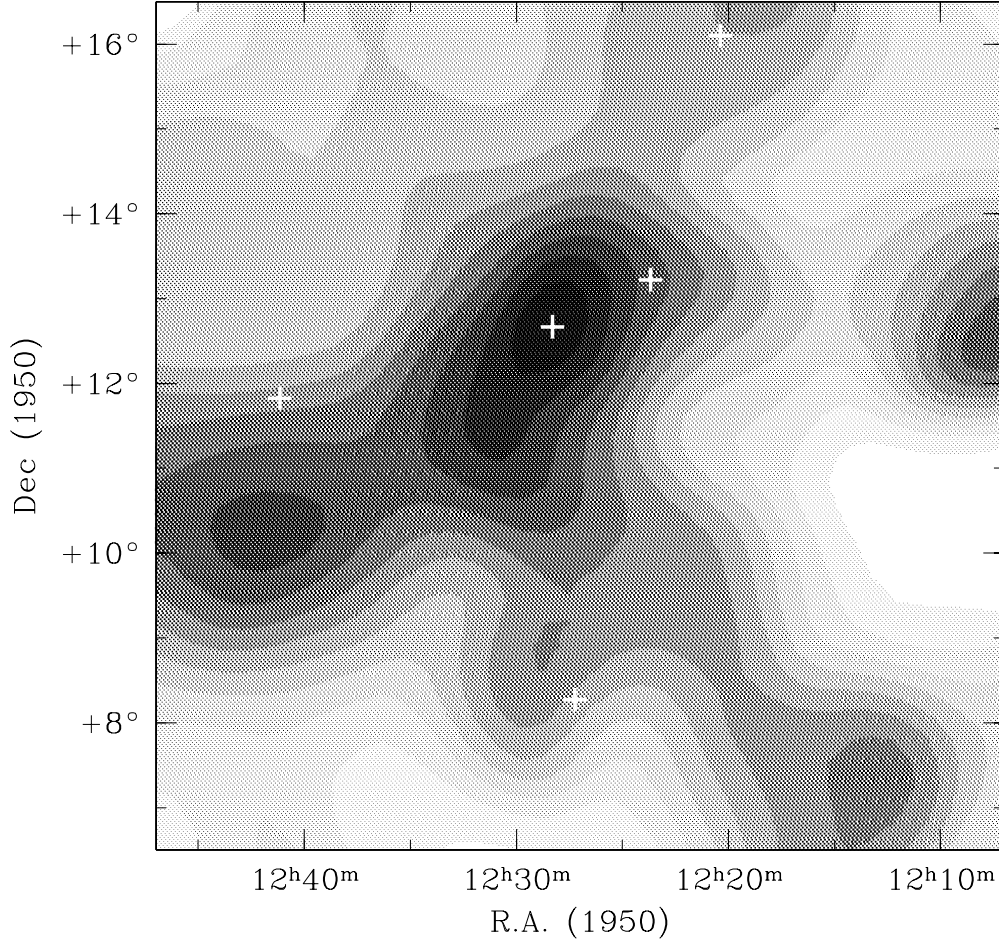


Figure 4: Greyscale image of the sky distribution of the HI deficiency in the central region of the Virgo cluster. The lightest regions in the maps correspond to  $\text{DEF} < 0.1$  and the darkest to  $\text{DEF} \geq 1.2$ . The contour spacing is linear. The peak value of HI deficiency coincides with the maximum of X-ray emission in the whole area. The positions of five dominant galaxies are marked by crosses (top to bottom: M100, M86, M87, M60, and M49).

formation rate in cluster galaxies—another property sensitive to environmental effects—shows signs of depression with respect to the field values at distances around twice the  $R_{200}$  “virial” radius. These two results seem to pose a problem for stripping mechanisms which require high environmental densities to be effective. The reduction of both the gas content and the star formation rate of these outer cluster galaxies can be achieved, however, if they are on strongly eccentric orbits that have carried them through the cluster center at least once (see Section 5). From the theoretical point of view, this possibility is supported by simulations of hierarchical structure formation<sup>4,5</sup> and by recent direct models of the origin of clustercentric gradients in the star formation rates within cold dark matter cosmogonies.<sup>6</sup>

## 2.2 The Virgo Cluster

The Virgo cluster is the nearest large-scale galaxy concentration which offers the possibility of exploring the manifestations of environmental effects on galaxies with greatest detail. Figure 4 shows the 2D adaptive map of the gas deficiency in the central region of this cluster (essentially

the classical Virgo I Cluster area). Several structures emerge clearly from the HI deficiency distribution. The zone with the maximum gas deficiency coincides with both the peak of X-ray emission and the main density enhancement, known as Cluster A. This is a double system comprising the subclusters centered on the giant ellipticals M87 and M86, which seem to be in the process of merging.<sup>7</sup> The radial nature of the HI deficiency pattern can also be observed in the greyscale map of the Virgo core. In spite of the irregular distribution of the galaxies, the shade intensity of this map grows toward the position of M87, where the density of the environment is highest. Five distinct gas-deficient patches appear to be radially connected with the central one. Two of them are located along the N-S direction: to the South, the HI deficiency extends towards the clump dominated by M49 (Cluster B); to the North, there is a mild increase of gas deficiency around the spiral M100. Along the EW axis, the distribution of HI deficiency is dominated by a region of strong gas depletion to the East. This EW asymmetry in the HI content has also been observed at X-ray wavelengths by Böhringer *et al.*,<sup>8</sup> who found that the faint Virgo X-ray emission can be traced out to a distance of  $\sim 5^\circ$ , except in the western side where the emission falls off more steeply. On the other hand, the position of the eastern local maximum of deficiency is located about one and a half degrees South of the peak of the density enhancement known as Cluster C around the pair of galaxies M59 and M60. Lumps of high HI-deficient galaxies are also found near the periphery of the surveyed region, where no X-ray gas is detected, in the areas of the background galaxy concentrations known as the M cloud in the NW, and the W' group and (northernmost part of the) W cloud in the SW. We speculate that these galaxy aggregates, which appear to be connected with the cluster center by gas-deficient zones, may have already experienced a first high-velocity passage through the Virgo core that could have affected the gas content of their galaxies and left behind a trail of gas-deficient objects, but that would have been insufficient to tear apart the densest portions of the lumps. It is also remarkable that the two zones having the lowest gas deficiency in our HI-deficiency maps—a small region to the East and South of M49 and a larger one mainly to the South of the M cloud—show a good positional correspondence with two infalling clouds composed almost entirely ( $\sim 80\%$ ) of spirals.<sup>9</sup>

### 3 HI Deficiency and Cluster Properties

The fact that the characteristics of our clusters vary widely suggests that it is worth investigating correlations between the overall degree of gas depletion and the global cluster properties that reflect the strength of the environmental perturbations on the gaseous disks. Figure 5 shows four X-ray parameters plotted against the fraction of spirals with  $\text{DEF} > 0.30$  found within  $1R_A$  of the cluster center,  $F_{\text{DEF}}$ , while in Figure 6 this fraction is compared with three optical properties. A fourth panel in this last figure compares the bolometric X-ray luminosity with the total spiral fraction. All plots involving the parameter  $F_{\text{DEF}}$  resemble essentially scatter diagrams with no significant correlations.

We recall at this point that suggestive though inconclusive indications of a trend toward greater HI-deficient fraction among clusters with high X-ray luminosity (in the 0.5–3.0 keV band) were found in the original investigation of Giovanelli and Haynes.<sup>10</sup> This relationship, however, is not corroborated with the present larger dataset. One reasonable explanation for the lack of any discernible correlation is the possible transmutation of some of the swept spirals into lenticulars, thereby weakening the relationships we are investigating by reducing the fraction of HI deficient galaxies to a greater degree for the strong X-ray clusters than for the weak ones. This possibility is suggested by the very strong anticorrelation shown by the total spiral fraction and the X-ray luminosity—the linear correlation coefficient  $r$  is less or equal than  $-0.90$  for all three wavebands—in the bottom right panel of Figure 6, implying that the fraction of lenticulars is correlated with X-ray luminosity.

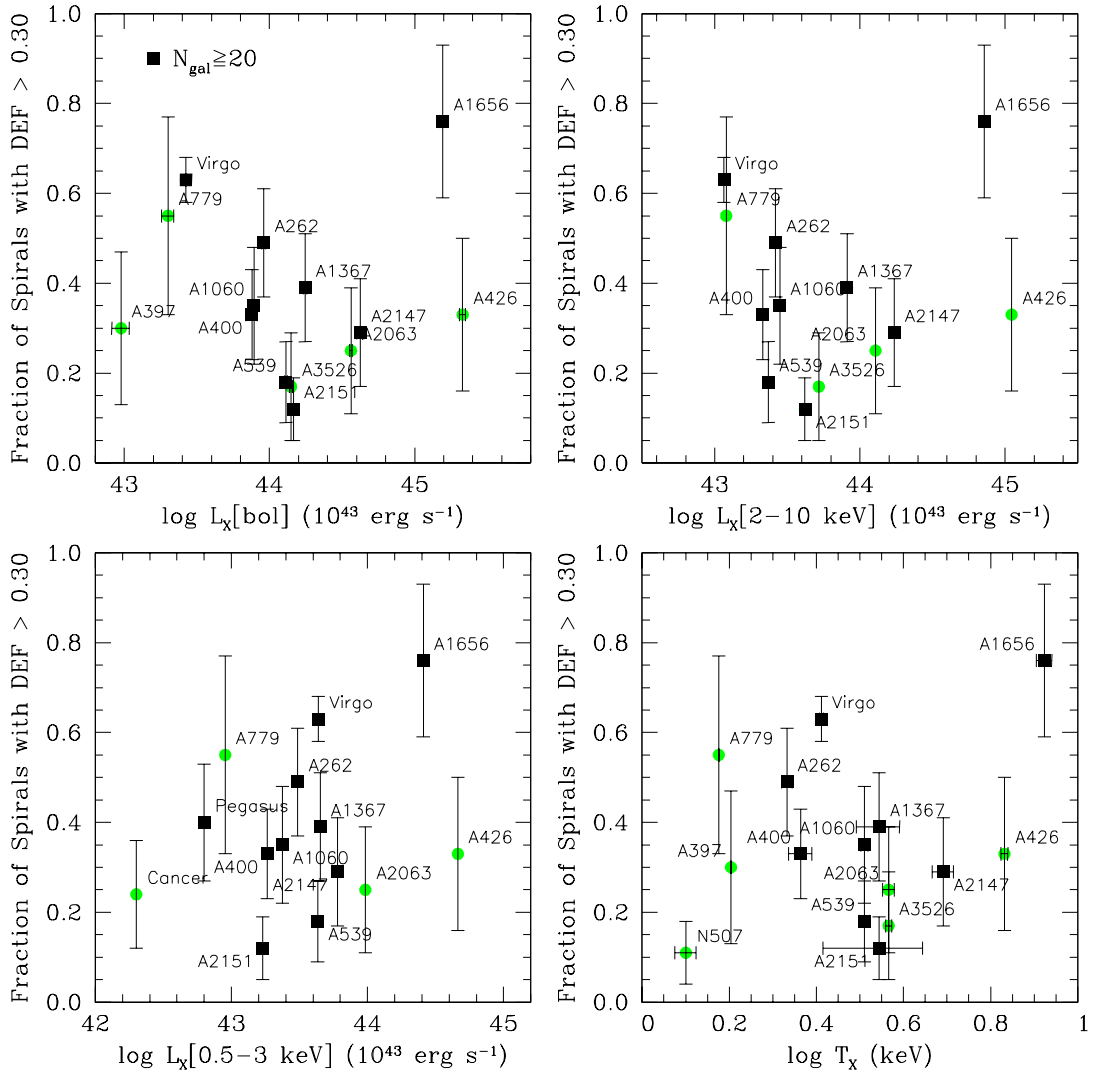


Figure 5: From left to right and top to bottom, spiral fraction within  $1R_A$  with a deficiency parameter DEF larger than 0.30 vs. cluster bolometric, 2–10 keV, and 0.5–3.0 keV X-ray luminosities, and cluster X-ray temperature. Square symbols identify clusters with a minimum of 20 objects in the central region.

One caveat that should be mentioned here is that possible selection effects and the incompleteness of some of our cluster galaxy samples might also explain the lack of good correlations between the fraction of HI-deficient spirals in clusters and the global properties of those systems. Note, for instance, that X-ray luminous clusters are more susceptible to incompleteness effects since they have a lower fraction of spirals. In an attempt to reduce the scatter of the plots, we have excluded from the analysis those samples containing fewer than 20 objects, which are the most likely affected by problems related to the small sample size. Systems in this restricted dataset certainly show signs of a possible relationship between  $F_{\text{DEF}}$  and the cluster X-ray luminosity in the 0.5–3.0 keV range ( $r = 0.55$ ), but there is no evidence for this trend in the other two X-ray windows. We argue that the results of the present exercise are not fully conclusive and require further investigation by means of still larger and more complete 21-cm-line investigation of galaxies in cluster fields.

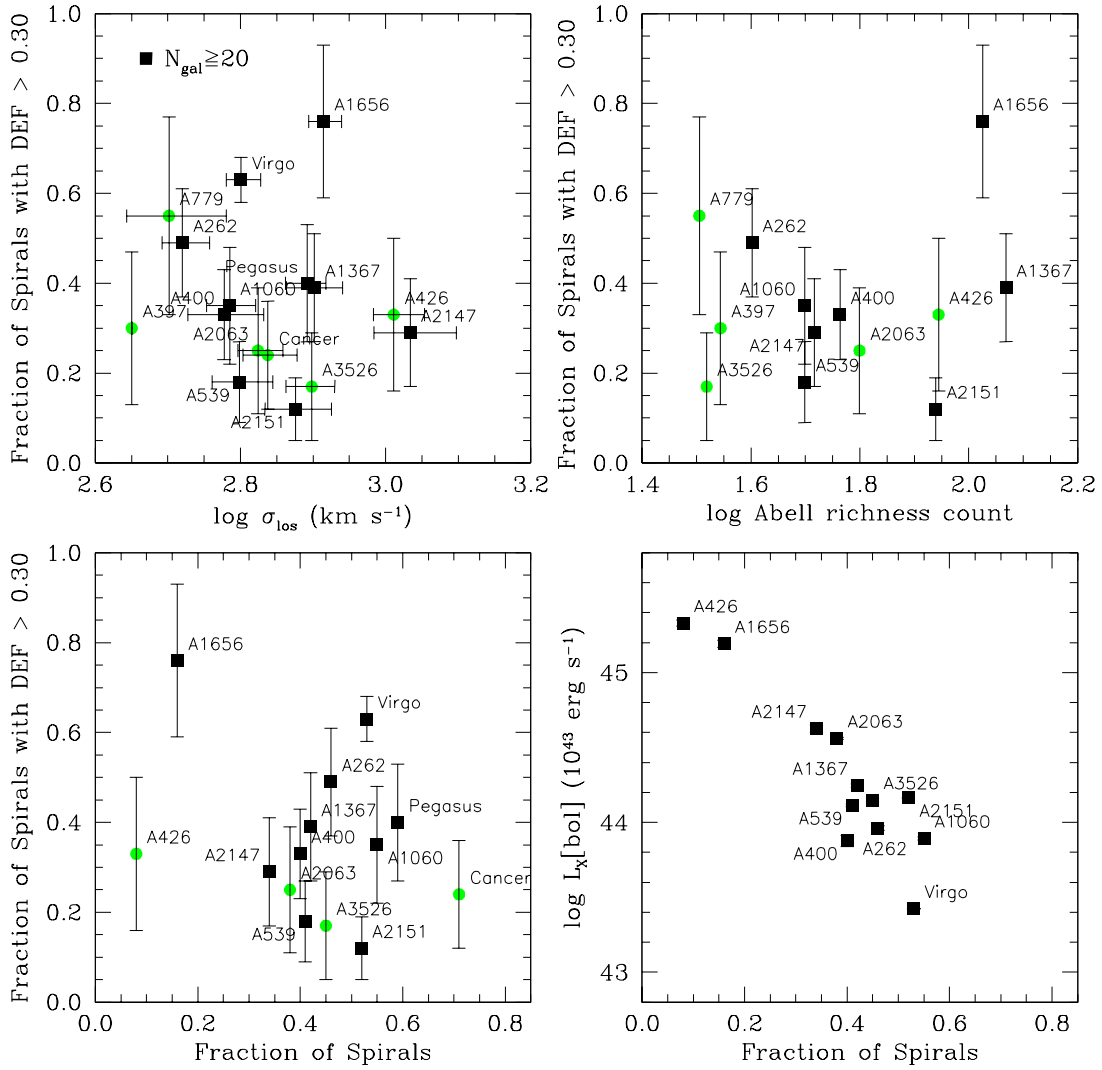


Figure 6: From left to right and top to bottom, spiral fraction within  $1R_A$  with a deficiency parameter DEF larger than 0.30 vs. cluster velocity dispersion, Abell richness count, and total fraction of spirals. The bottom right panel shows the bolometric X-ray luminosity plotted against the total fraction of spirals.

#### 4 The Variation of HI Deficiency with Morphological Type

Earlier studies of HI deficient spirals in clusters<sup>11,15</sup> have found indications of an increase of the gaseous deficiency towards early galaxy types. In order to investigate the existence of a gas deficiency-morphology relationship, we present in the top panels of Figure 7 the bar charts of the percentage of galaxies inside  $1R_A$  at a given morphology with deficiency parameter DEF > 0.30 in the Virgo and the composite samples. Comparison of the two bar charts shows, in the first place, that the Virgo cluster exhibits a notably larger fraction of gas-deficient galaxies for any given morphological class, a result which is simply due to the fact that we are sampling farther down the HI mass function in Virgo than in the more distant clusters. Differences in the normalization aside, the plots confirm that for a spiral, the likelihood of being HI deficient depends on its morphology. Both the Virgo and the composite cluster sample share a common pattern: a roughly gradual descent of the fraction of HI-deficient galaxies as the Hubble type goes from Sa to Sc, by a total amount of  $\sim 40\%$ , which levels off for the latest types. The

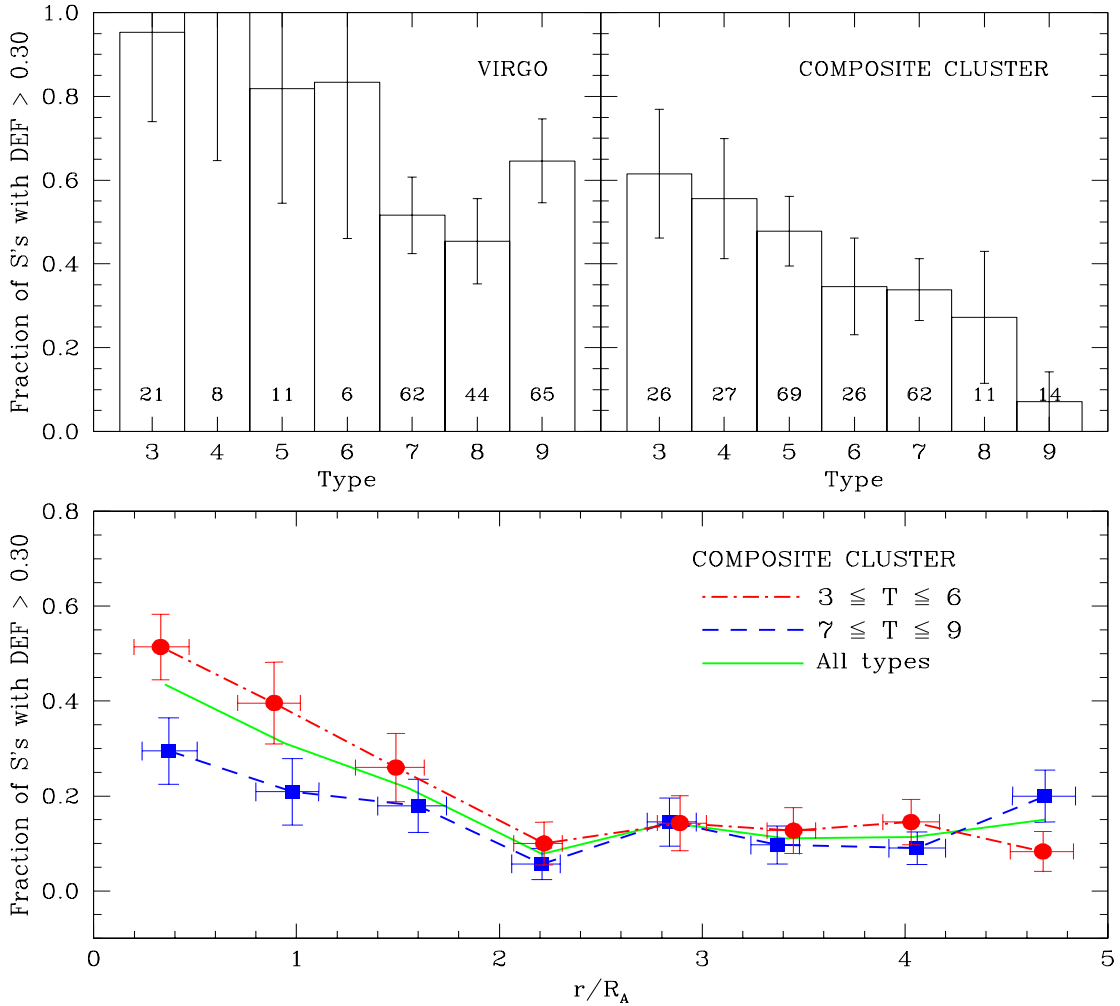


Figure 7: *Top*: fraction of galaxies within  $1R_A$  with deficiency parameter  $DEF > 0.30$  as a function of the morphological type for the Virgo sample (left) and a composite cluster sample formed by combining the rest of the HI-deficient systems (right). Hubble types have been replaced by a numerical code which runs from  $T = 3$  for Sa's to  $T = 9$  for Sd-Sm and irregular galaxies. The numbers within each bin indicate the total number of galaxies in that bin. *Bottom*: same as in the upper panel of Figure 2, for the early (circles) and late (squares) spirals separately. The solid curve reproduces the trend of the entire spiral population.

only discrepancy arises in the very latest morphology bin, which shows a noticeable recovery of the deficiency fraction for Virgo and a sharp drop for the composite cluster (we assign more credibility to the Virgo data since very gas-poor dwarf galaxies are underrepresented in the more distant clusters). We want to stress also that the distributions of values of the parameter  $DEF$  separately by morphological type demonstrate that the earliest spirals, as well as the dwarfs, are not only more likely to be deficient in HI than the intermediate disks, but they also have a higher gas deficiency.

On the other hand, the bottom panel of Figure 7 demonstrates that the observed correlation between HI deficiency and morphology is not simply a consequence of the well-known morphological segregation of cluster galaxies. In this plot, we reproduce the radial run of the HI-deficient fraction for the composite HI-deficient cluster sample but separating the early ( $T: 3 \div 6$ ) and late ( $T: 7 \div 9$ ) spiral type subsets. From this graph one sees: 1) that inside the region of influence of the cluster environment, early-type galaxies have systematically higher gas deficiencies, *at*

any projected radius, than the late types; and 2) that the difference between the HI-deficient fractions of the early- and late-type populations increases gradually towards the cluster center. Identical results, although with more abrupt radial variations due to the spatial lumpiness of the cluster, are found for the Virgo sample. These results lead to the conclusion that the observed correlation of HI deficiency and morphology is not a secondary effect of the spatial segregation of the galaxies, but reflects the interplay between the intrinsic characteristics of these objects and the physical mechanism behind HI depletion.

## 5 HI Deficiency and Galaxy Orbits

The hypothesis that HI-deficient galaxies lose their interstellar HI at small distances from cluster cores but can still be found at large radial distances suggests that the HI-deficient objects follow highly eccentric orbits. Information on the eccentricity of galaxy orbits can be extracted from the radial run of the line-of-sight (los) velocity dispersion.

In Figure 8, we show, separately for the Virgo and composite clusters, the mean radial profiles of the normalized los velocity dispersion,  $\sigma_{\text{los}}^*$ , for six different galaxian subpopulations. For the composite HI-deficient cluster, we see that the velocity dispersion for the spirals with the strongest gas deficiencies ( $\text{DEF} \geq 0.48$ ) drops significantly in a manner consistent with radial orbits.<sup>11</sup> The curve for the gas-rich objects ( $\text{DEF} \leq 0$ ) decreases too with increasing radius, although the decline is sensibly weaker than for the gas-deficient galaxies. These results suggest that one possible explanation for the relationship found in the previous section between disk morphology and gas content could be that early spirals have an orbital distribution more radially anisotropic than late types. To test this possibility, we have inferred the velocity dispersion profiles of the spirals subdivided into early and late disks. Again, we find indications of radial orbits for these two broad morphological groupings, although the trajectories of the galaxies in the first group does not seem to be more eccentric than those in the second: if anything there is a hint for the opposite effect. Not surprisingly, the kinematic behavior of the entire spiral population is intermediate among those shown by all the previous subdivisions. On the other hand, the earliest Hubble types, i.e. lenticulars and ellipticals, show a lower and almost constant velocity dispersion profile compatible with an isotropic distribution of velocities. This finding is yet another manifestation of the well-known fact that S and E+S0 galaxies do not share the same kinematics: late-type galaxies are likely recent arrivals to the virialized cluster cores, which consist essentially of ellipticals and lenticulars.<sup>12</sup> In addition to supporting this basic picture, our data also indicate that a segregation has developed among the orbits of the infalling spirals according to their gaseous contents since the objects with the more eccentric trajectories, *regardless of morphology*, reach deeper into the cluster cores and are thus more efficiently stripped of their neutral hydrogen.

The same analysis for the Virgo cluster galaxies is reproduced in the top panel of Figure 8. We see that, to a first approximation, the velocity dispersion profiles corresponding to all the galaxy subgroups are essentially flat (notice, for instance, the curve exhibited by the entire spiral population), although with a noticeably positive excess of the velocity dispersion of the spirals relative to the E+S0 population. Given that Virgo is a dynamically young galaxy system, we interpret these results as indicative of the fact that the trajectories of the spiral galaxies within the central region of this cluster are strongly perturbed by large and rapid fluctuations of the mean gravitational field caused by the ongoing merger of major subclumps. Because of this large-scale phase mixing, environmental influences on the disks have not yet been capable of inducing a neat orbital segregation between gas-poor and gas-rich objects. The presence of high-velocity gas-poor objects at relatively large clustercentric distances would result from the spirals that populate the outskirts of the infalling clouds and that, still bound to these systems, have been scattered with high velocities to large apocenter orbits during the merger process.

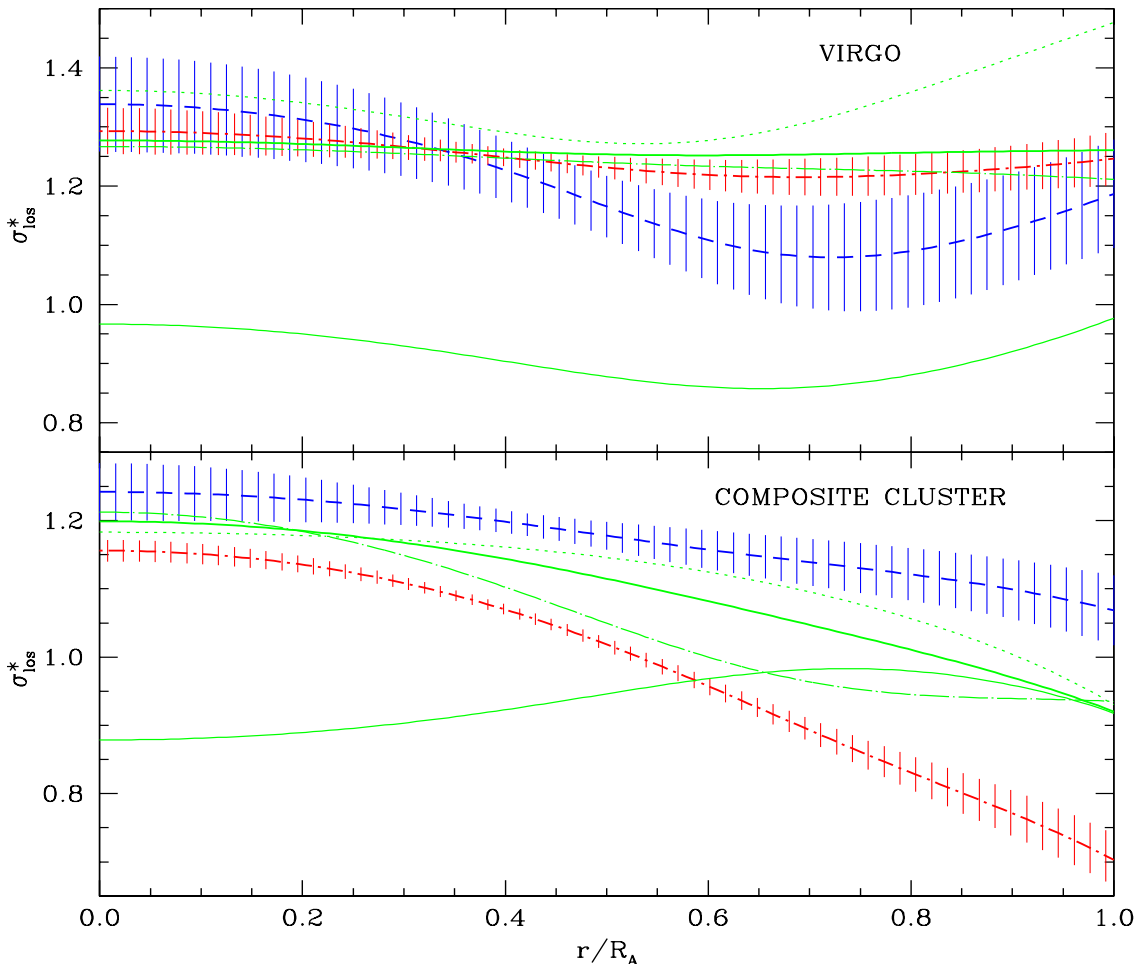


Figure 8: Radial run of the *normalized* los velocity dispersion up to  $1R_A$  for the Virgo (top) and the composite HI-deficient cluster (bottom). The observed peculiar velocities of the individual galaxies have been scaled to the average los velocity dispersion of their parent cluster. Line coding is as follows: thick dot-dash for spirals with  $\text{DEF} \geq 0.48$ , thick dash for spirals with  $\text{DEF} \leq 0$ , thick solid for all spirals, dots for early spirals, dot-long dash for late spirals, and solid for ellipticals and lenticulars. Only error bars for the curves of the spirals with extremal HI contents are displayed for clarity.

## 6 Implications of the Results on the Mechanism of HI Depletion

The natural consequence of gas losses as radical as our results indicate would be—provided gas replenishment does not occur at exceptionally high rates—a reduction in the star-formation activity of the galaxy, followed by the fading of the disk and the consequent increase of the bulge to disk ratio (B/D). This prediction is in good agreement with the decline of disk luminosity and the invariance of bulge brightness with increasing local density observed in the spirals of rich clusters.<sup>13</sup> Also quite consistent with this idea is the finding by Koopmann and Kenney<sup>14</sup> that objects in Virgo classified as Sa have similar B/D's than the Sc's and only differ in their overall star formation rates which are strongly reduced in the outer disk. The morphological transformation of the swept galaxies into S0-like objects could be completed through the suppression of the spiral features by continued disk heating by tidal encounters. Of course, the possible morphological evolution of cluster spirals towards earlier types has serious difficulties in explaining the presence of S0's in the field. While some stripped galaxies may have fairly radial orbits that carry them at large distances from the cluster centers, one must bear in mind

that not all the lenticular galaxies, outside and inside clusters, arise necessarily from HI-deficient spirals.

The present investigation provides clear evidences of the strong influence that the cluster environment has on the gaseous disks of spirals. The marked radial pattern of HI deficiency indicates that galaxies lose their gas near the cluster centers. This result is consistent with the finding that spirals with substantial HI deficiency follow orbits with large radial components. It appears then, that the stripping of gas requires high IGM densities and relative velocities. The detection of galaxies with extreme HI deficiencies, but still retaining their spiral morphology, suggests also that the stripping of the atomic hydrogen is a relatively recent event in the life of these objects. Furthermore, the details of the relationship between HI deficiency and morphology are consistent with the idea that some galaxian characteristics directly related to the Hubble type, such as for instance the presence of central depressions in the HI disks, enhance the efficiency of gas removal. According to these results, ISM-IGM interactions, basically ram pressure supplemented by the accompanying effects of viscosity and turbulence, are favored over other environmental mechanisms as the main cause of gas depletion in clusters.

## References

1. M.P. Haynes and R. Giovanelli, *Astronomical Journal* **89**, 758 (1984)
2. J.M. Solanes, R. Giovanelli, and M.P. Haynes, *Astrophysical Journal* **461**, 609 (1996)
3. M.L. Balogh, D. Schade, S.L. Morris, H.K.C. Yee, R.G. Carlberg, and E. Ellingson, *Astrophysical Journal* **504**, L75 (1998)
4. S. Ghigna, B. Moore, F. Governato, G. Lake, T. Quinn, and J. Stadel, *Monthly Notices of the Royal Astron. Soc.* **300**, 146 (1998)
5. A.C. Ramírez, and R.E. de Souza, *Astrophysical Journal* **496**, 693 (1998)
6. M.L. Balogh, J.F. Navarro, and S.L. Morris, astro-ph/0004078 (2000)
7. S. Schindler, B. Binggeli, and H. Böhringer, *Astronomy & Astrophysics* **343**, 420 (1999)
8. H. Böhringer, U.G. Briel, R.A. Schwarz, W. Voges, G. Hartner, and J. Trümper, *Nature* **368**, 828 (1994)
9. G. Gavazzi, A. Boselli, M. Scodreggio, D. Pierini, and E. Belsole, *Monthly Notices of the Royal Astron. Soc.* **304**, 595 (1999)
10. R. Giovanelli and M.P. Haynes, *Astrophysical Journal* **292**, 404 (1985)
11. A. Dressler, *Astrophysical Journal* **301**, 35 (1986)
12. L. Sodré, Jr., H.V. Capelato, J.E. Steiner, and A. Mazure, *Astronomical Journal* **97**, 1279 (1989)
13. J.M. Solanes, E. Salvador-Solé, and M. Sanromá, *Astronomical Journal* **98**, 798 (1989)
14. R.A. Koopmann and J.D.P. Kenney, *Astrophysical Journal* **497**, 75 (1998)
15. P. Chamaraux, C. Balkowski, and P. Fontanelli, *Astronomy & Astrophysics* **165**, 15 (1986)